Journal of Inorganic Biochemistry 191 (2019) 174–182

Contents lists available at ScienceDirect

Journal of Inorganic Biochemistry

journal homepage: www.elsevier.com/locate/jinorgbio

Structure – activity relationships of 2-quinolinecarboxaldehyde thiosemicarbazone gallium(III) complexes with potent and selective anticancer activity

Wanbao Cao[a], Jinxu Qi[a], Kun Qian[a], Liang Tian[a], Zhen Cheng[b], Yihong Wang[a,*]

[a] School of Chemistry and Chemical Engineering, Southeast University, Nanjing 211189, China
[b] Stanford Cancer Institute, Member of Academic Council, Stanford University, USA

ARTICLE INFO

Keywords:
2-Quinolinecarboxaldehyde thiosemicarbazone
Gallium(III) complex
Anticancer activity
Metallodrugs

ABSTRACT

Six gallium(III) complexes (Ga1–Ga6) with 2-quinolinecarboxaldehyde thiosemicarbazone analogues were synthesized and characterized. These gallium(III) complexes exhibited potent anticancer activity and exceeded that of the corresponding metal free ligands. Importantly, these gallium(III) complexes have a strong selectivity for tumor cells. Through the study of cellular mechanisms, we have found that the lipophilicity of ligands is closely linked to the antitumor activity of gallium(III) complexes. Additionally, we have chosen Ga6 with the best anti-tumor activity to study the mechanism of apoptosis. Caspase-3 and 9 activation and Annexin V-FITC/Propidium iodide (PI) dual-staining studies revealed that Ga6 promote apoptosis in A549 cells lines. Ga6 induces intracellular reactive oxygen species (ROS) and disrupts mitochondrial membrane potential.

1. Introduction

Platinum-based agents are extensively employed to treat a variety of malignant tumor and achieve great success after FDA approved, such as cisplatin, carboplatin, and oxaliplatin, but platinum-based anticancer drugs have some limitations including toxicity for normal cells and multifactorial resistance [1–3]. Therefore, continuous research and development of novel organometallic anticancer agents is of great significance, for example, gallium(III) thiosemicarbazone complexes, ruthenium(II) polypyridyl complexes and benzimidazole-based iridium (III) complexes [4–6]. Notably, gallium is the second metal after platinum to be applied in cancer treatment, since the FDA has approved gallium nitrate injection as a Phase II clinical drug for non-hodgkin lymphoma [7–9]. However, studies have shown that the toxicity of gallium is mainly due to the gallium easily to hydrolyze and form hydroxide in vivo circulation, which greatly affects their apply in anticancer chemotherapy [10]. In order to improve this disadvantage, many gallium complexes are synthesized and evaluated in vitro and in vivo, such as tris(maltolato)gallium(III), tris(8-quinolinolato)gallium(III) (KP46), phenolate-based gallium(III) and thiosemicarbazone-based gallium(III) complexes [10,11].

α-*N*-heterocyclic thiosemicarbazones have been extensively investigated as metal chelators in anticancer agents design [12,13]. These compounds and their derivatives have been shown wide range of pharmacological properties, such as antibacterial, antiviral and antineoplastic activity [14–16]. Previous studies have demonstrated that thiosemicarbazones derivatives are potent antiproliferative agents, such as aminopyridinecarbaldehyde thiosemicarbazones, dipyridylketone thiosemicarbazones and hydroxyquinoline thiosemicarbazones in vitro and in vivo [16–18]. Quinoline thiosemicarbazones scaffold contain the inherent NNS tridentate coordination system, and the N and S atoms are able to act as “soft” electron donors and chelate gallium(III) ions to form cytotoxic metal complexes [19–21]. Furthermore, coordination gallium with QTs forming complexes can prevent the formation of gallium hydroxide and improve their bioavailability and anticancer activity.

Mitochondria are the main site of energy production and aerobic respiration of cells, and they also play key roles in essential cellular processes, such as intrinsic apoptosis regulation and intracellular signaling [22–24]. Mitochondrial dysfunction is related to various cancers, therefore, many mitochondrial-targeted chemotherapeutic agents are applied in cancer treatment [25,26]. ROS elevation and mitochondrial dysfunction are closely related events. Accumulation of large amounts of ROS could collapse mitochondrial membrane potential, resulting in increased mitochondrial outer membrane permeability, then apoptosis-related proteins were allow to enter the cytoplasmic matrix, promoting apoptosis [25,27].

Here, we synthesized and characterized a series of novel 2-quinolinecarboxaldehyde thiosemicarbazones gallium complexes. The

* Corresponding author at: 2 Southeast Road, Nanjing 211189, China.
E-mail address: yihongwang@seu.edu.cn (Y. Wang).

https://doi.org/10.1016/j.jinorgbio.2018.11.017
Received 6 August 2018; Received in revised form 23 November 2018; Accepted 25 November 2018
Available online 28 November 2018
0162-0134/

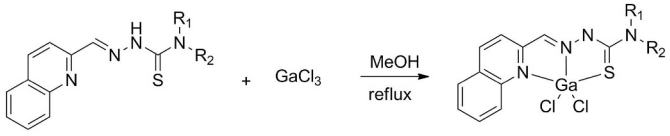

Ga1: R1 = H, R2 = H; Ga2: R1 = Me, R2 = H;
Ga3: R1 = Me, R2 = Me; Ga4: R1 = Et, R2 = Et;
Ga5: R1NR2 = pyrrolyl; Ga6: R1NR2 = piperidyl;

Scheme 1. Synthesis routes for L1–L6 and Ga1–Ga6.

structure−activity relationships of these gallium(III) complexes were examined. To assess the potential anticancer mechanism of gallium complexes, we have investigated their antiproliferative activity, apoptosis analysis, cell cycle, intracellular ROS, mitochondrial membrane potential and activated apoptotic proteins.

2. Results and discussion

2.1. Synthesis, characterization and crystallography description

The tridentate ligands containing 2-quinolinecarboxaldehyde pharmacophores and thiosemicarbazones group for the coordination to Ga (III) were synthesized according to the previous report [28,29]. Ligands L1–L6 were prepared straightly forward via Schiff base condensation reactions and did not require further purification. Ga(III) complexes were synthesized by the coordination of ligands with gallium(III) chloride (molar ratio of 1:1). All of gallium complexes were crystallized from the methanol solution with high purity without further purification. The synthetic routes to Ga(III) complexes (Ga1–Ga6) are shown in Scheme 1. Ligands L1–L6 and complexes Ga1–Ga6 were characterized by ^{1}H NMR spectroscopy (Figs. S1–S12 of the Supporting information) and elemental analysis.

In the ^{1}H NMR spectra of L1–L6 the signals of N−NH−C were found in the δ 11.20–11.80, respectively, which is in accordance with hydrogen bonding to the oxygen of DMSO and with the presence of the ligands in the E configuration. However, no signal was observed for N−NH−C in the spectra of Ga(III) complexes, indicating that the ligands were protonated after coordination. The piperidyl hydrogens shifted significantly upon coordination and formation of Ga(III) complexes.

The structure of 1:1 ligand/Ga(III) complex (Ga6) was determined by single-crystal X-ray diffraction (Fig. 1), and the crystal data and structure refinement were showed in Table 1. The selected interatomic distances (Å) and angles (°) were shown in Table 2. Ga6 crystallized in the monoclinic system and space group $P2_1/c$. There are two Cl atoms (Cl1 and Cl2) and one ligand (S1, N1 and N2) coordinated to Ga(III) metal center, which lead to a distorted trigonal bipyramidal geometry (Fig. 1). The Ga1−N1 bond lengths of Ga6 (2.207 Å) is slightly longer than that of Ga1−N2 (2.029 Å). The length of Ga1−Cl1 (2.1960 Å) and Ga1−Cl2 (2.2084 Å) bond are similar. The bond of Ga1−S1 (2.3475 Å) is the longest among these coordination bonds. The N1−Ga1−S1 bond angle is 159.19°, which is close to 160°.

Table 1
Crystal data and structure refinement for Ga6.

Identification code	Ga6
Empirical formula	$Ga1_6H_{17}Cl_2GaN_4S$
Formula weight	438.01
Temperature/K	296.15
Crystal system	Monoclinic
Space group	$P2_1/c$
a/Å, b/Å, c/Å	15.9102(11), 9.0431(5), 12.7572(10)
α/°, β/°, γ/°	90, 100.641(7), 90
Volume/Å^3	1803.9(2)
Z	4
Radiation	MoKα (λ = 0.71073)
Index ranges	$-18 \le h \le 8$, $-10 \le k \le 10$, $-14 \le l \le 15$
Goodness-of-fit on F^2	1.033
Final R indexes [all data]	$R_1 = 0.0426$, $wR_2 = 0.0844$
CCDC no.	1852606

Table 2
Selected interatomic distances and angles for Ga6.

Atom-atom	Length/Å	Atom-atom-atom	Angle/°
Ga(1)−S(1)	2.3475(8)	Cl(1)−Ga(1)−S(1)	99.22(3)
Ga(1)−Cl(1)	2.1960(9)	Cl(1)−Ga(1)−Cl(2)	117.18(3)
Ga(1)−Cl(2)	2.2084(7)	Cl(1)−Ga(1)−N(1)	92.19(6)
Ga(1)−N(2)	2.029(2)	Cl(2)−Ga(1)−S(1)	98.47(3)
Ga(1)−N(1)	2.207(2)	N(2)−Ga(1)−S(1)	82.20(6)
		N(2)−Ga(1)−Cl(1)	119.02(6)
		N(2)−Ga(1)−Cl(2)	122.87(6)
		N(2)−Ga(1)−N(1)	77.04(8)
		N(1)−Ga(1)−S(1)	159.19(6)
		N(1)−Ga(1)−Cl(2)	91.61(6)

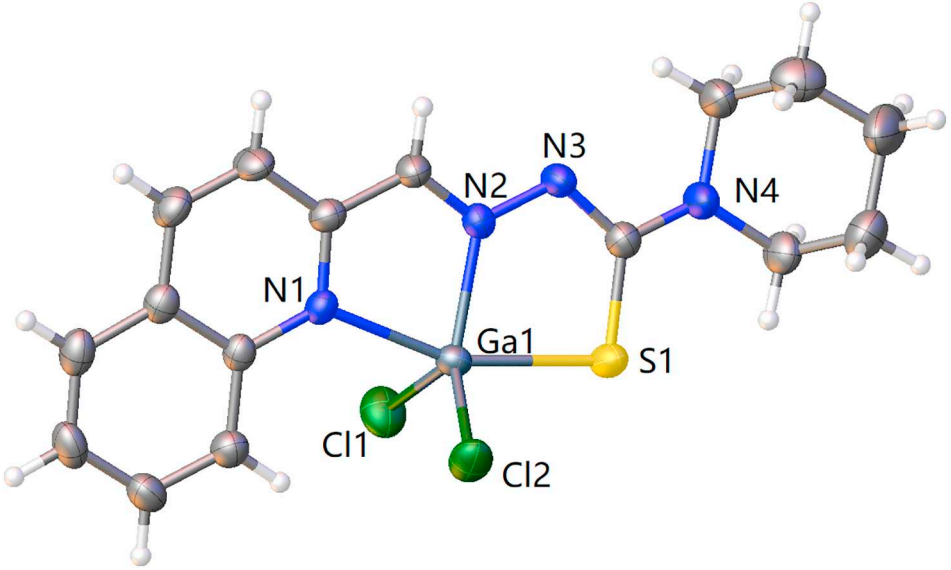

Fig. 1. Molecular structure of Ga6 showing the environment about the Ga(III) atom.

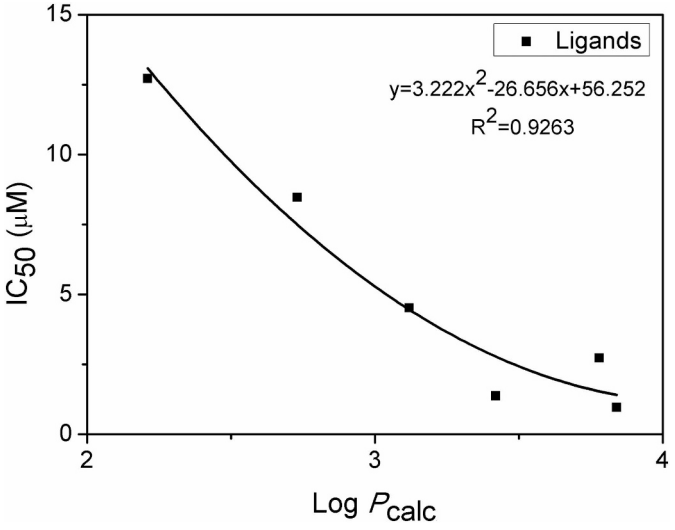

Fig. 2. Relationship between the antiproliferative activity (IC_{50}) and lipophilicity (log P_{calc}) of the ligands using A549 cells. Lines were fitted using OriginPro 8.

2.2. Antiproliferative activity of the ligands and gallium(III) complexes

We evaluated the anticancer properties of thiosemicarbazone ligands and Ga(III) complexes on two malignant cancer cell lines and human normal cell line: SGC7901 human gastric cancer cell line, A549 human lung cancer cell line and LO2 human normal liver cells. A number of important structure-activity relationships are considered in the design of anticancer agents. The ligands and gallium complexes showed more active with the increase of the lipids of the terminal-N substituents (Fig. 2). All of the thiosemicarbazone ligands and Ga(III) complexes have a higher antiproliferative activity for these selected malignant cancer cell lines. All of the synthetic compounds showed lower cytotoxicity for LO2 (> 50 μM) than cancer cell lines.

The concentrations of the studied compounds which kill 50% of SGC7901, A549 and LO2 cells (IC_{50}) are listed in Table 3. All ligands and Ga(III) complexes showed low toxicity for human normal liver cells LO2. Ligands (L1–L6) as well as their Ga(III) complexes were highly active against malignant cancer cells. Ga(III) complexes show stronger cytotoxicity than metal-free ligands in malignant cancer cells, indicating enhanced activity after the coordination of gallium. The antitumor activity of the Ga(III) complexes (Ga1–Ga6) increases with the lipophilicity of the ligand. In all compounds, Ga6 has the best antitumor activity, and the IC_{50} value for A549 and SGC7901 is 0.46 μM and 0.66 μM, respectively.

Table 3
IC_{50} values of ligands and Ga(III) complexes toward cell lines for 48 h.

	IC_{50} (μM)		
	A549	SCG-7901	LO2
L1	12.71 ± 0.55	19.92 ± 0.77	> 50
L2	8.47 ± 0.32	10.88 ± 0.49	> 50
L3	4.52 ± 0.35	5.53 ± 0.38	> 50
L4	2.73 ± 0.27	5.26 ± 0.34	> 50
L5	1.37 ± 0.06	3.82 ± 0.11	> 50
L6	0.96 ± 0.03	1.93 ± 0.14	> 50
Ga1	1.41 ± 0.45	5.43 ± 0.67	> 50
Ga2	0.93 ± 0.46	3.97 ± 0.31	> 50
Ga3	0.86 ± 0.32	2.65 ± 0.25	> 50
Ga4	0.61 ± 0.27	1.29 ± 0.09	> 50
Ga5	0.52 ± 0.11	0.85 ± 0.13	> 50
Ga6	0.46 ± 0.03	0.66 ± 0.05	30.86 ± 1.22

2.3. Cellular uptake of Ga in A549 cells

The rate of uptake of exogenous drugs by cells is an important manifestation of their bioavailability and affects drugs biological activity [30–32]. We measured Ga content in a549 cells treated with $GaCl_3$ and Ga1–Ga6 in order to evaluate whether 2-quinolinaldehyde thiosemicarbazone ligands promote cellular uptake. Treatment of A549 cells with Ga1–Ga6 for 12 h resulted in a significant increase in the cell concentration of Ga compared with $GaCl_3$-treated cells, indicating that 2-quinolinaldehyde thiosemicarbazone Ga(III) complexes are easily drawn into the cells (Fig. 3).

2.4. Cell cycle analysis

Cell cycle is tightly correlated with the proliferation and development of cancer cells [33–35]. The cytotoxicity of many anticancer drugs is often associated with cell cycle perturbation. To evaluate whether the complex could induce apoptosis, A549 cells were double-stained with PI after 48 h of L6 and Ga6 co-incubation, and analyzed by flow cytometry (Fig. 4). After the 24 h co-incubation of L6 or Ga6, the percentage of G2 phase cells decreased 2.29% and 12.64% than vehicle control-treated, respectively (Fig. 4D). This outcome indicated that the coordination of the ligand with gallium could inhibit the G2/M transition in the cell cycle.

2.5. Apoptosis analysis

Apoptosis (programmed cell death) is the orderly death of genes controlled by cells that maintain internal stability [36–38]. However, apoptosis is often suppressed in cancer cells, so activation of apoptosis is an effective antitumor strategy [39]. To evaluate whether the complex could induce apoptosis, A549 cells were double-stained with AnnexinV/PI after 48 h of L6 or Ga6 co-incubation, and analyzed by flow cytometry. Quantification of the result indicate that L6 and Ga6 were found to be 12.89% and 31.6% more effective than vehicle control-treated (Fig. 5). Ga6 is > 2-fold as active as L6, almost 6-fold more potent than the control group in A549 cells. The result of apoptosis assay demonstrated that the Ga(III) complex had more activity of promoting cell apoptosis than metal-free ligand, which was consistent with MTT assay.

2.6. Intracellular ROS measurement

In normal conditions, the intracellular antioxidant system can maintain the metabolic balance of ROS [40]. However, the interventions of some exogenous drug may lead to intracellular ROS or decreased scavenging capacity of cells [41,42]. To evaluate whether the Ga(III) complex can induce intracellular ROS increase, A549 cells were stained by a fluorescent probe (DCFH-DA) after 48 h of L6 or Ga6 co-incubation, and analyzed by flow cytometry (Fig. 6A). Quantification of the DCF fluorescence peaks indicate that L6 and Ga6 were found to be 55.3% and 121.3% more effective than vehicle control-treated (Fig. 6B). The result demonstrated that the Ga(III) complex significantly increase the intracellular ROS. Intracellular ROS overload can inhibit the proliferation of cells in G1, S and G2 phase, and G2/M phase arrest is related to the process of defense against oxidative damage and anti-apoptosis.

2.7. Mitochondrial membrane potential analysis

Intracellular ROS overload may cause mitochondrial dysfunction [43,44]. Mitochondrial membrane potential (ΔΨm) is an important indicator of mitochondrial function [22,45]. Normal mitochondrial membrane potential is required to maintain mitochondrial oxidative phosphorylation and ATP production, which is necessary to maintain mitochondrial function [23,24]. An important change in apoptosis is

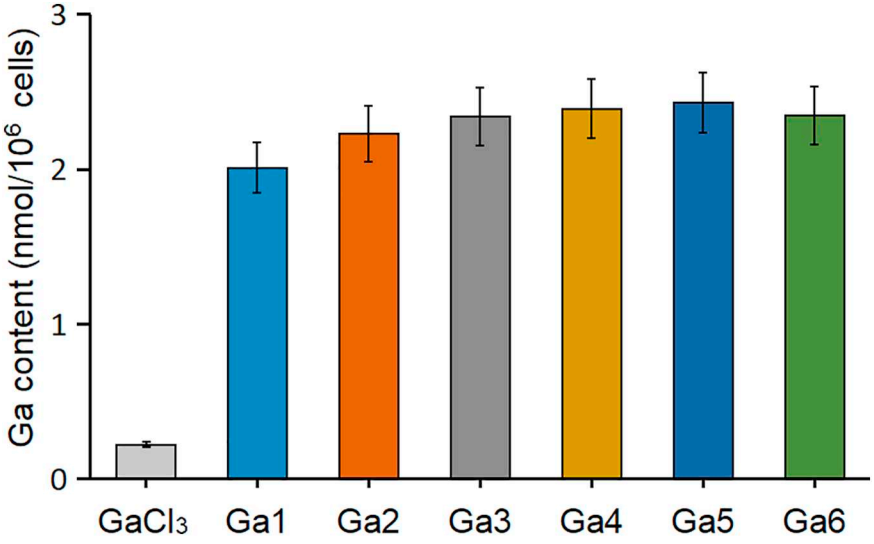

Fig. 3. Cellular uptake of Ga in A549 cells. A549 cells were incubated with 10.0 μM of $GaCl_3$ and Ga1–Ga6 for 12 h at 37 °C, respectively.

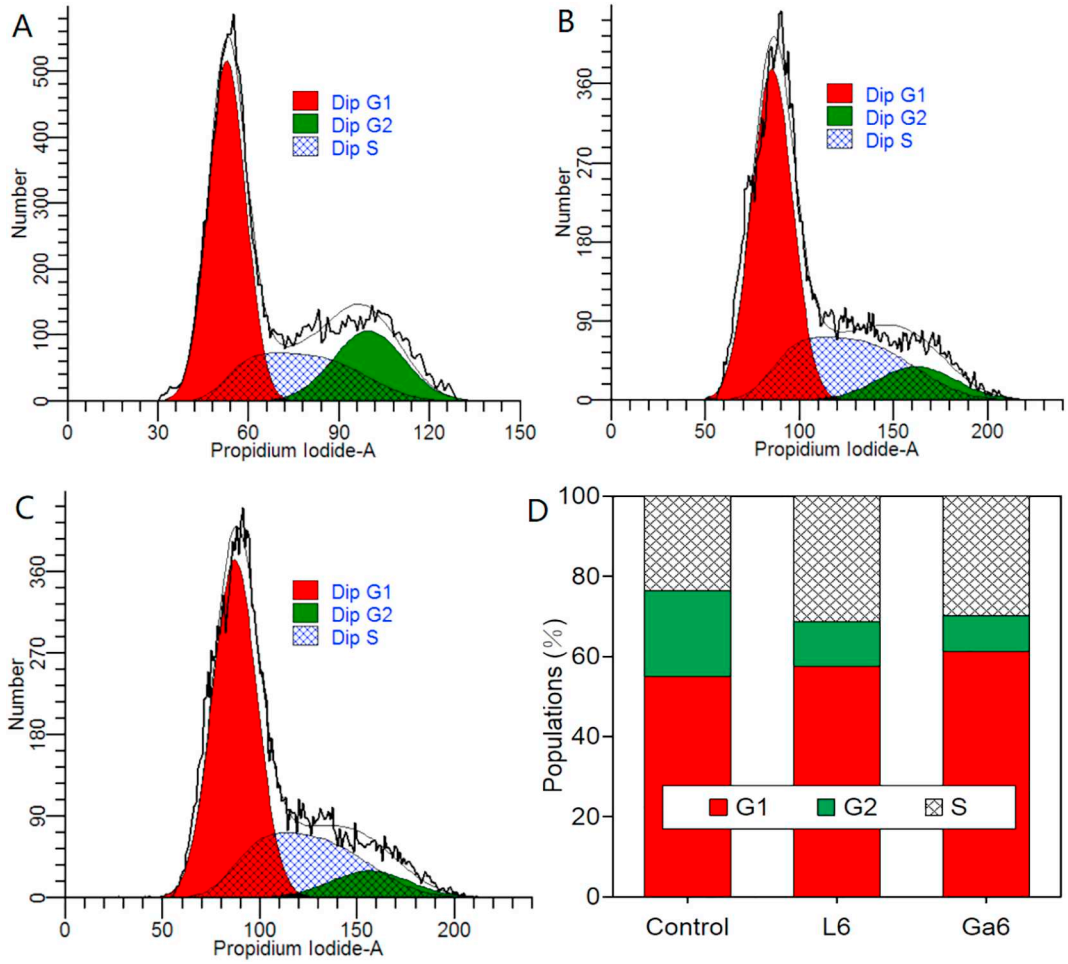

Fig. 4. A549 cells were treated with vehicle control (A), L6 (B), and Ga6 (C), at the indicated concentrations, after which they were stained with PI and analyzed by flow cytometry. (D) Populations for cell cycle distribution.

the collapse of mitochondrial membrane potential [22]. To evaluate whether the Ga(III) complex can induce the collapse of mitochondrial membrane potential, A549 cells were stained by JC-1 fluorescent probe (5,5′,6,6′-tetrachloro-1,1′,3,3′-tetraethyl-imida-carbocyanineiodide) after 48 h of L6 or Ga6 co-incubation, and analyzed by flow cytometry (Fig. 7). The presence of JC-1 in the form of polymer (red fluorescence) means that the mitochondrial membrane potential is high; When JC-1 exists in monomer form (green fluorescence), it means that mitochondrial membrane potential collapse. We can observe that the mitochondria of the control cells present red fluorescence, while L6 or

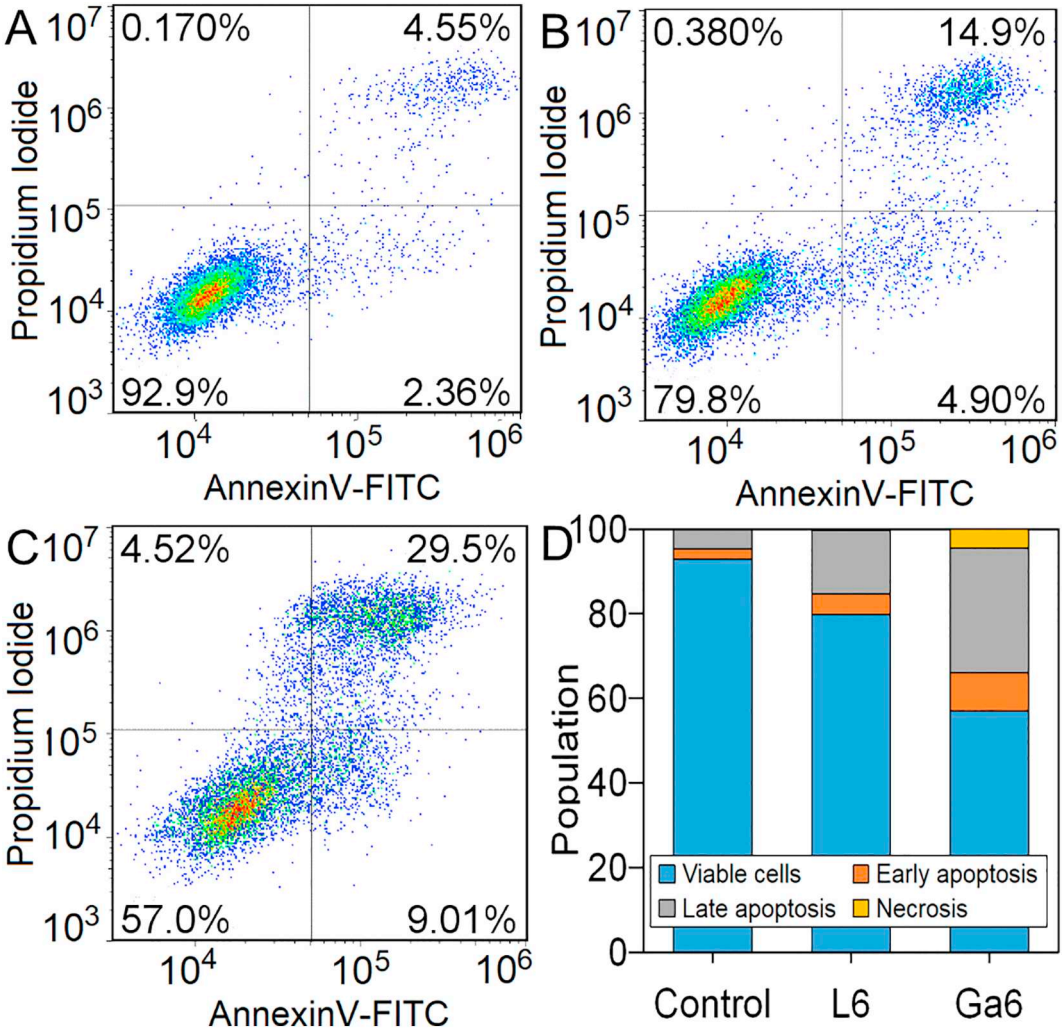

Fig. 5. Effect of the cell apoptosis. Quantification of Annexin V and PI double-stained A549 cells after treatment with (A) vehicle control, (B) L6, (C) Ga6 for 24 h at the indicated concentrations by flow cytometric. (D) Populations for cell apoptosis.

Ga6-treated cells emerge green fluorescence (Fig. 7), which indicates that the collapse of the mitochondrial transmembrane potential in the intervention of Ga(III) complex.

2.8. The activation of caspase-3 and 9 affected by Ga(III) complexes

The dissipation of mitochondrial membrane potential may increase mitochondrial membrane permeability, thereby lead to the release of apoptosis factors [46,47]. Thus, we analyzed the influence of Ga(III) complexes on the activation of caspase-3 and 9 in A549 cells by flow cytometry (Fig. 8). After incubated with L6 or Ga6 for 24 h, the activated caspase-3 protein levels increased to 8% and 26.3%, the activated caspase-9 protein levels increased to 9.6% and 25.7%, respectively (Fig. 8). These results show that Ga(III) complex is more potent activators of caspase-3 and 9 than the corresponding ligand.

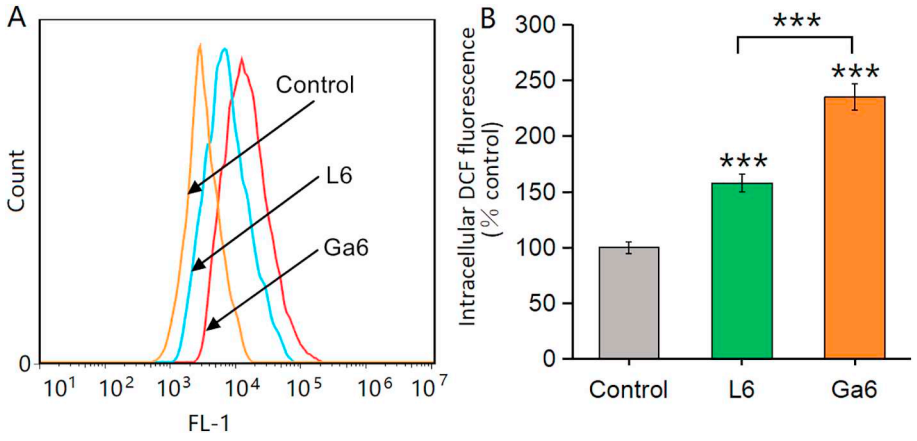

Fig. 6. (A) Intracellular ROS was detected in A549 cells after treatment with vehicle control, L6, and Ga6 for 24 h; (B) quantification of the flow cytometric results in (A) showing the percentage of cells with increased intracellular DCF oxidation compared to control cells. Results are the mean ± SD (n = 3): *p < 0.05, **p < 0.01, ***p < 0.001.

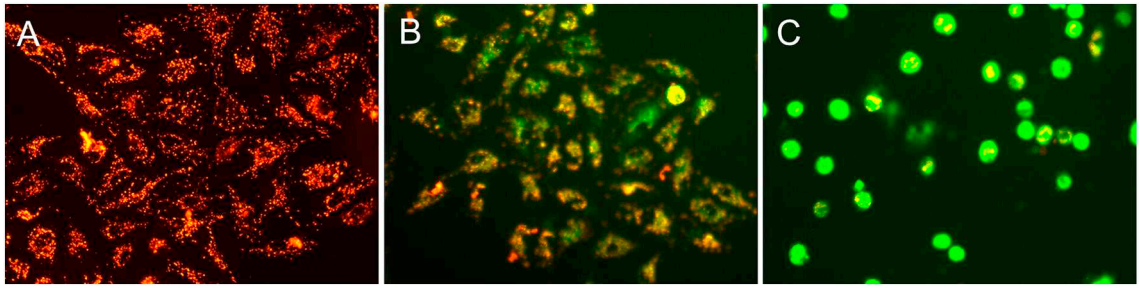

Fig. 7. Assay of A549 cells mitochondrial membrane potential with JC-1 as fluorescence probe staining method. (A) Control, (B) L6, and (C) Ga6.

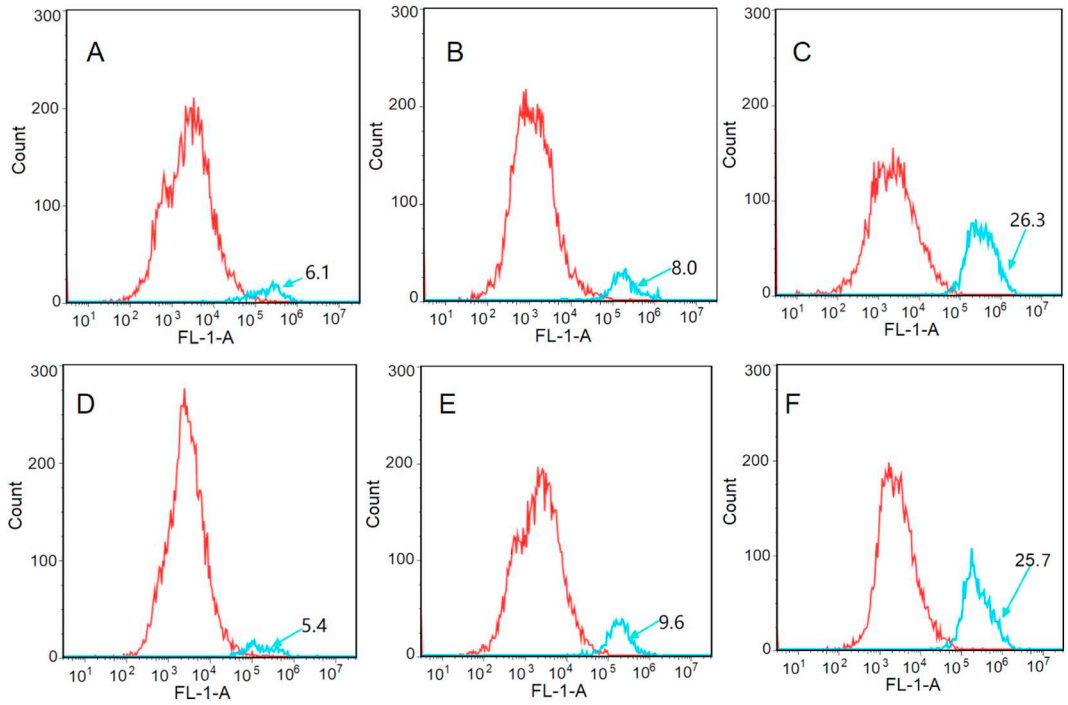

Fig. 8. Activation levels of caspase-3 protein in A549 cells treated with 10 μM of (A) control, (B) L6, and (C) Ga6; activation levels of caspase-9 protein in A549 cells treated with 10 μM of control (D) control, (E) L6, and (F) Ga6.

3. Conclusions

We demonstrated that a series of 2-quinolinecarboxaldehyde thiosemicarbazone gallium(III) complexes have higher cell cytotoxicity compared to the corresponding metal-free ligand alone. In addition, ligands and Ga(III) complexes have less effect on normal cells (LO2) than malignant cancer cells. The ligands significantly promote the cellular utilization of gallium(III) trichloride through coordinate with gallium(III). The structure-activity relationship shows that modification of lipophilic groups on ligands significantly increase the antitumor activity of gallium(III) complexes. The G2 phase of the cell cycle is significantly shortened with the intervention of gallium(III) complex. Gallium(III) complex also induce apoptosis through increasing intracellular ROS leave, disrupting mitochondrial membrane potential and activating caspase family proteins. In conclusion, the gallium (III) complex has great potential and can be developed as a new candidate drug for treating cancer.

4. Experimental

4.1. Materials and methods

Gallium chloride, 2-quionlinecarboxaldehyde and thiosemicarbazides were purchased from Innochem Company (Shanghai, China). Other chemicals and solvents were analytically pure. Water was reaction distillated before use. The A549, SGC7901 and LO2 cell lines were purchased from Chinese academy of sciences.

4.2. Synthesis and characterization of L1–L6

The thiosemicarbazone ligands were synthesized by condensation reaction of the proper thiosemicarbazide with 2-quionlinecarboxaldehyde. Thiosemicarbazide (1 mmol) was dissolved in warm ethanol (10 mL) and added solution of 2-quionlinecarboxaldehyde (1 mmol) in ethanol (10 mL). Then added 4 drops of glacial acetic acid. The mixture was heated under reflux for 4–5 h to form a bright yellow solution. The precipitate was subsequently filtered when the mixture solution was cooled to room temperature, washed with cold ethanol and dried under vacuum.

2-(2-Quinolinylmethylene)hydrazinecarbothioamide (L1): light yellow solid, yield 67%. Anal. Calcd ($C_{11}H_{10}N_4S$): C, 57.40; H, 4.35; N, 24.35. Found: C, 56.37; H, 4.38; N, 26.33. ^{1}H NMR (600 MHz, DMSO-d_6), δ 11.82 (s, 1H, N−NH−C), 7.76, 7.95, 8.20, 8.33, 8.42, 8.46 (m, 6H, quinoline-H), 7.58 (s, 1H, N=CH), 7.95 (s, 2H, C−NH_2). ESI - MS *m/z* (%) 230.06 (M − H, 100).

2-*N*-methyl-2-(2-quinolinylmethylene)hydrazinecarbothioamide (L2): light yellow solid, yield 72%. Anal. Calcd ($C_{12}H_{12}N_4S$): C, 58.99; H, 4.95; N, 22.93. Found: C, 56.96; H, 4.98; N, 24.95. ^{1}H NMR

(600 MHz, DMSO-d_6). δ 11.89 (s,1H, N—NH—C), 7.99, 8.01, 8.24, 8.41, 8.46, 8.82 (m, 6H, quinoline-H), 7.63 (s, 1H, N═CH), 7.78 (s, 1H, C—NH), 3.08 (s, 3H, N—CH_3). ESI - MS *m/z* (%) 244.08 (M − H, 100).

***N,N*-dimethyl-2-(2-quinolinylmethylene)hydrazinecarbothioamide (L3)**: light yellow solid, yield 77%. Anal. Calcd ($C_{13}H_{14}N_4S$): C, 60.44; H, 5.46; N, 21.69. Found: C, 60.46; H, 5.45; N, 20.70. ^{1}H NMR (600 MHz, DMSO-d_6). δ 11.82 (s, 1H, N—NH—C), 7.77, 7.97, 8.01, 8.20, 8.37, 8.56 (m, 6H, quinoline-H), 7.62 (s, 1H, N═CH), 3.35 (s, 6H, CH_3—N—CH_3). ESI - MS *m/z* (%) 258.09 (M − H, 100).

***N,N*-diethyl-2-(2-quinolinylmethylene)hydrazinecarbothioamide (L4)**: yellow solid, yield 82%. Anal. Calcd ($C_{15}H_{18}N_4S$): C, 62.91; H, 6.34; N, 19.56. Found: C, 60.34; H, 5.38; N, 21.57. ^{1}H NMR (600 MHz, DMSO-d_6). δ 12.13 (s, 1H, N—NH—C), 7.79, 7.99, 8.02, 8.41, 8.51, 9.51 (m, 6H, quinoline-H), 7.63 (s, 1H, N═CH), 3.71 (m, 4H, N—CH_2), 1.19 (m, 6H, —CH_3). ESI - MS *m/z* (%) 286.13 (M − H, 100).

1-Pyrrolidinecarbothioic acid 2-(2-quinolinylmethylene)hydrazide (L5): yellow solid, yield 80%. Anal. Calcd ($C_{15}H_{16}N_4S$): C, 63.35; H,5.67; N, 19.70. Found: C, 63.08; H, 5.65; N, 18.69. ^{1}H NMR (600 MHz, DMSO-d_6). δ 11.44 (s, 1H, N—NH—C), 7.78, 7.98, 8.01, 8.02, 8.35, 8.37 (m, 6H, quinoline-H), 7.62 (s, 1H, N═CH), 3.82 (m, 4H, N—CH_2), 1.93 (m, 4H, CH_2—CH_2). ESI - MS *m/z* (%) 284.11 (M − H, 100).

1-Piperidinecarbothioic acid 2-(2-quinolinylmethylene)hydrazide (L6): yellow solid, yield 76%. Anal. Calcd ($C_{16}H_{18}N_4S$): C, 64.40; H, 6.08; N, 18.78. Found: C, 67.38; H, 6.79; N, 16.59. ^{1}H NMR (600 MHz, DMSO-d_6). δ 11.30 (s, 1H, N—NH—C), 7.77, 7.97, 8.02, 8.03, 8.35, 8.52 (m, 6H, quinoline-H), 7.60 (s, 1H, N═CH), 3.36 (m, 4H, N—CH_2), 2.50, 2.49 (m, 6H, CH_2—CH_2). ESI - MS m/z (%) 298.13 (M − H, 100).

4.3. Synthesis and characterization of the complexes Ga1–Ga6

1 mmol of ligand was dissolved in anhydrous methanol (10 mL), resulting in an yellow solution. An equimolar amount of gallium (III) chloride dissolved in methanol (10 mL) was added. The mixture was gently refluxed for 30 min. Cooling to room temperature, the yellow solution was volatilized slowly. A few days later, single crystals of gallium complexes were obtained by filtrating. The gallium complexes were separated, washed several times with methanol and dried under vacuum.

[2-(2-Quinolinylmethylene)hydrazinecarbothioamide-*N,N,S*-gallium(III)] bis(Chloride) (Ga1): yellow solid, yield 82%. Anal. Calcd ($C_{11}H_{10}N_4SGaCl_2$): C, 35.62; H, 2.72; N, 15.11. Found: C, 34.65; H, 3.63; N, 16.10. ^{1}H NMR (600 MHz, DMSO-d_6). δ 7.76, 8.12, 8.17, 8.23, 8.62, 8.69 (m, 6H, quinoline-H), 7.91 (s, 1H, N═CH), 5.16 (s, 2H, C—NH_2). EI - MS *m/z* (%) 367.92 (M − CH_3, 100).

[*N*-methyl-2-(2-quinolinylmethylene) hydrazinecarbothioamide-*N,N,S*-gallium(III)] bis(Chloride) (Ga2): yellow solid, yield 78%. Anal. Calcd ($C_{12}H_{12}N_4SGaCl_2$): C, 37.44; H, 3.14; N, 14.56. Found: C, 38.88; H, 3.82; N, 13.84. ^{1}H NMR (600 MHz, DMSO-d_6). δ 7.77, 7.78, 8.18, 8.33, 8.436, 8.76 (m, 6H, quinoline-H), 8.15 (s, 1H, N═CH), 7.31 (s, 1H, C—NH), 3.08 (s, 3H, N—CH_3). EI - MS *m/z* (%) 381.93 (M − CH_3, 100).

[*N,N*-dimethyl-2-(2-quinolinylmethylene)hydrazinecarbothioamide-*N,N,S*-gallium(III)] bis(Chloride) (Ga3): red solid, yield 77%. Anal. Calcd ($C_{13}H_{14}N_4SGaCl_2$): C, 39.14; H, 3.54; N, 14.04. Found: C, 37.15; H, 3.99; N, 15.38. ^{1}H NMR (600 MHz, DMSO-d_6). δ 7.52, 7.76, 8.14, 8.18, 8.61, 9.07 (m, 6H,quinoline-H), 7.92 (s, 1H, N═CH), 4.07 (s, 6H, CH_3—N—CH_3). EI - MS *m/z* (%) 395.95 (M − CH_3, 100).

[*N,N*-diethyl-2-(2-quinolinylmethylene)hydrazinecarbothioamide-*N,N,S*-gallium(III)] bis(Chloride) (Ga4): red solid, yield 85%. Anal. Calcd ($C_{15}H_{18}N_4SGaCl_2$): C, 42.19; H, 4.25; N, 13.12. Found: C, 42.93; H, 4.02; N, 12.71. ^{1}H NMR (600 MHz, DMSO-d_6). δ 7.77, 7.94, 8.16, 8.79, 8.86, 9.27 (m, 6H, quinoline-H), 7.99 (s, 1H, N═CH), 3.76 (m, 4H, N—CH_2), 1.22 (m, 6H, —CH_3). EI - MS *m/z* (%) 423.98 (M − CH_3, 100).

[1-Pyrrolidinecarbothioic acid 2-(2-quinolinylmethylene) hydrazide-*N,N,S*-gallium(III)] bis(Chloride) (Ga5): red solid, yield 80%. Anal. Calcd ($C_{15}H_{16}N_4SGaCl_2$): C, 42.39; H, 3.79; N, 13.18. Found: C, 43.52; H, 3.29; N, 13.01. ^{1}H NMR (600 MHz, DMSO-d_6). δ 7.79, 7.87, 8.11, 8.29, 8.92, 9.36 (m, 6H, quinoline-H), 8.06 (s, 1H, N═CH), 3.77 (m, 4H, N—CH_2), 2.07 (m, 4H, CH_2—CH_2). EI - MS *m/z* (%) 421.97 (M − CH_3, 100).

[1-Piperidinecarbothioic acid 2-(2-quinolinylmethylene) hydrazide-*N,N,S*-gallium(III)] bis(Chloride) (Ga6): red solid, yield 85%. Anal. Calcd ($C_{16}H_{18}N_4SGaCl_2$): C, 43.77; H, 4.13; N, 12.76. Found: C, 42.49; H, 4.85; N, 11.72. ^{1}H NMR (600 MHz, DMSO-d_6). δ 7.77, 7.97, 8.18, 8.76, 8.84, 9.26 (m, 6H, quinoline-H), 8.00 (s, 1H, N═CH), 3.96 (m, 4H, N—CH_2), 1.63, 1.60 (m, 6H, CH_2—CH_2). EI - MS m/z (%) 435.98 (M − CH_3, 100).

4.4. Determination of structure of gallium(III) complex (Ga6)

X-ray single crystal diffraction data of Ga6 were collected at room temperature on a Bruker SMART ApexII CCD diffractometer using graphite-monochromatized MoKα radiation (λ = 0.71073 Å). Final unit cell parameters were based on the fitting of all reflections positions (SADABS). The structure was solved by direct methods and refined on F^2 by full-matrix least-squares using the SHELX-97 program. Hydrogen atoms were placed in geometrically ideal positions and constrained to ride on their parent atoms by direct methods. Crystal data, data collection procedure, structure determination methods and refinement results are summarized in Table 1. Molecular graphics was obtained from ORTEP (Fig. 1).

4.5. Cytotoxicity analysis (MTT)

Human non-small cell lung cancer cell line A549, human gastric cancer cell line SGC7901 and human normal liver cells LO2 were cultured as recommended at 37 °C in a humidified atmosphere of 5% CO_2 and 95% air in a Thermo Fisher Incubator. 10 mM stock solutions of ligands and gallium(III) complexes were prepared in DMSO and diluted in fresh medium for use. The final concentration of DMSO never exceeded 0.1% (v/v). Cells were seeded into 96-well plate and incubated for 24 h at 37 °C, 5% CO_2 and 95% air. Then the medium was replaced with the respective medium containing ligands or Ga (III) complexes at different concentrations and incubated for 48 h. 10 μL of MTT was added and the medium was removed after 4 h of incubation. Finally, crystal violet was solubilized in 100 μL DMSO and the absorbance was measured at 570 nm. IC_{50} values were determined by the standard method. These assays were conducted in triplicate.

4.6. Uptake of Ga(III) complexes in cells

A549 cells (1×10^7 cells) were treated with 10 μM Ga1–Ga6 and $GaCl_3$, respectively, for 12 h at 37 °C, 5% CO_2 and 95% air. Cold PBS (phosphate buffer, pH = 7.4) were used for rinsing the cells for three times after being collected. Cells were lysed in 1 M NaOH (1 mL) and diluted with 2% (v/v) HNO_3 (5 mL) to determine whole cell gallium content. The amount of gallium taken up by the cells was determined by ICP-MS. The instrument calibrates gallium using a standard solution containing 10, 50, 100, 500 and 1000 ppb gallium.

4.7. Cell cycle analysis

1 mL of 1×10^6 cells/mL A549 cells were cultured in 70 mm culture dishes at least 12 h, then treated with 10 μM of L6 or Ga6 for 24 h. Cells were collected and washed three times in cold PBS, and then fixed with 75% cold ethanol overnight at −20 °C. The fixed cell washed with cold PBS, stained with propidium iodide for 30 min, and then analyzed by flow cytometry. For each sample, 10,000 events were recorded. Data

analysis was performed by FlowJo software. These assays were conducted in triplicate.

4.8. Cell apoptosis analysis

1 mL of 1×10^6 cells/mL A549 cell line was cultured in 96-well plate and left for attachment overnight at 37 °C in a CO_2 incubator. The cells were then treated with the respective IC_{50} doses of L6 or Ga6, then incubated for 12 h. Cell apoptosis was determined by Annexin V and PI staining according to the manufacturer's protocol for the Annexin V: FITC Apoptosis Detection Kit (Becton Dickinson). The cells were then harvested and washed with ice-cold PBS three times, then resuspended with 100 μL of AnnexinV-binding buffer (2.5 mM $CaCl_2$, 140 mM NaCl, 10 mM Hepes/NaOH, pH = 7.4). Then 5 mL each of annexin V and PI were added to these samples. Finally, these samples were incubated for 15 min at room temperature and then analyzed by flow cytometry. These assays were conducted in triplicate.

4.9. The measurement of intracellular ROS

Intracellular ROS generation of A549 cells was measured using Reactive oxygen species assay kit. 2 mL of 1×10^6 cells/mL cells were induced with 20 μM of L6 or Ga6 at 37 °C for 1 h, serum free medium washed twice. DCFH-DA could pass through the cell membrane to produce DCFH by hydrolysis of the intracellular esterase. Intracellular reactive oxygen species (ROS) can oxidize DCFH to produce fluorescent DCF. Therefore, the detection of DCF fluorescence could inform us of the level of intracellular reactive oxygen species. The cells were incubated in 2 mL of serum free medium containing H_2DCF-DA (2 μM) for 30 min at 37 °C, serum free medium washed twice. Cells were collected and assayed by flow cytometric analysis (Becton Dickinson), and ten thousand events were collected for every sample. The DCF fluorescence peaks for these cell samples were evaluated and quantified by FlowJo software.

4.10. The change of mitochondrial membrane potential assay

Mitochondrial membrane potential analysis was determined by fluorescent dye JC-1 staining according to the manufacturer's protocol for the JC-1 assay kit. In brief, 2 mL of 1×10^6 cells/mL cells were treated with 10 μM of L6 or Ga6 in 6-well plates for 1 h. Cells were harvested and washed three times with PBS after 24 h of incubation. Then cells were stained with 1 mL of JC-1 stock solution (10 mg/mL). Assays were initiated by incubating A549 cells with JC-1 for 30 min at 37 °C in the dark and detected with a flow cytometry. The date of cell apoptosis was analyzed by FlowJo software. These assays were conducted in triplicate.

4.11. The measurement of pro-apoptotic proteins assay

Intracellular pro-apoptotic protein caspase-3 generation of A549 cells was measured using CaspGLOW™ Fluorescein Active Caspase-3 Staining Kit (BioVision). Briefly, 2 mL of 1×10^6 cells/mL cells were induced with 10 μM of L6 or Ga6, caspase inhibitor Z-VAD-FMK [Benzyloxycarbonyl-Val-Ala-Asp(OMe)-fluoromethylketone] (1 mL/mL) and vehicle (0.1% DMSO) at 37 °C for 1 h, respectively. Aliquot 300 mL each of the induced and control cultures into Eppendorf tubes. Add 1 mL of FITC-DEVD-FMK into each tube and incubate for 0.5 h at 37 °C incubator with 5% CO_2. Centrifuge cells at 3000 rpm for 5 min and remove supernatant. Resuspend cells in 0.5 mL of Wash Buffer, and centrifuge twice. Resuspending cells in 300 mL of Wash buffer for flow cytometric analysis (FACScan, Becton Dickinson, San Jose, CA). Keep samples on ice. Analyzing samples by flow cytometry using the FL-1 channel. The fluorescence peaks for these cell samples were evaluated and quantified by FlowJo software. These assays were conducted in triplicate.

4.12. Statistical analysis

Data were reported as means ± SD (number of experiments). All tests were performed in triplicates with full agreement between the results. The statistical significance was assessed using Student's *t*-test.

Conflict of interest

The authors declare that they have no conflict of interests.

Acknowledgements

This work was supported by National Natural Science Foundation of China (81571812), Priority Academic Program Development of Jiangsu Higher Education Institutions (1107047002), the Fundamental Research Funds for the Central Universities and Postgraduate Research & Practice Innovation Program of Jiangsu Province (KYCX17_0135). The research was also supported by the Scientific Research Foundation of Graduated School of Southeast University (YBJJ1787).

Appendix A. Supplementary data

All relative data of the experiment have been deposited into Supplementary Information. Supplementary data to this article can be found online at https://doi.org/10.1016/j.jinorgbio.2018.11.017.

References

[1] W. Fiebiger, U. Olszewski, E. Ulsperger, K. Geissler, G. Hamilton, Clin. Transl. Oncol. 13 (2011) 43–49.
[2] P. Collery, A. Mohsen, A. Kermagoret, J. D'Angelo, G. Morgant, D. Desmaele, A. Tomas, T. Collery, M. Wei, A. Badawi, Anticancer Res. 32 (2012) 2769–2781.
[3] T.C. Johnstone, K. Suntharalingam, S.J. Lippard, Chem. Rev. 116 (2016) 3436–3486.
[4] M.R. Kaluđerović, S. Gómez-Ruiz, B. Gallego, E. Hey-Hawkins, R. Paschke, G.N. Kaluđerović, Eur. J. Med. Chem. 45 (2010) 519–525.
[5] C.S. Burke, A. Byrne, T.E. Keyes, J. Am. Chem. Soc. 140 (2018) 6945–6955.
[6] H. Na, T.S. Teets, J. Am. Chem. Soc. 140 (2018) 6353–6360.
[7] C.R. Chitambar, Curr. Opin. Oncol. 16 (2004) 547–552.
[8] M.A. Jakupec, B.K. Keppler, Curr. Top. Med. Chem. 4 (2004) 1575–1583.
[9] M. Yang, C.R. Chitambar, Free Radic. Biol. Med. 45 (2008) 763–772.
[10] C.R. Chitambar, W.E. Antholine, Antioxid. Redox Signal. 18 (2013) 956–972.
[11] K.D. Mjos, J.F. Cawthray, E. Polishchuk, M.J. Abrams, C. Orvig, Dalton Trans. 45 (2016) 13146–13160.
[12] D.B. Lovejoy, D.M. Sharp, N. Seebacher, P. Obeidy, T. Prichard, C. Stefani, M.T. Basha, P.C. Sharpe, P.J. Jansson, D.S. Kalinowski, P.V. Bernhardt, D.R. Richardson, J. Med. Chem. 55 (2012) 7230–7244.
[13] J. Qi, S. Liang, Y. Gou, Z. Zhang, Z. Zhou, F. Yang, H. Liang, Eur. J. Med. Chem. 96 (2015) 360–368.
[14] J. Tian, D.M. Peehl, W. Zheng, S.J. Knox, Cancer Lett. 298 (2010) 231–237.
[15] J. Qi, Y. Gou, Y. Zhang, K. Yang, S. Chen, L. Liu, X. Wu, T. Wang, W. Zhang, F. Yang, J. Med. Chem. 59 (2016) 7497–7511.
[16] A.E. Stacy, D. Palanimuthu, P.V. Bernhardt, D.S. Kalinowski, P.J. Jansson, D.R. Richardson, J. Med. Chem. 59 (2016) 8601–8620.
[17] A. Popović-Bijelić, C.R. Kowol, M.E.S. Lind, J. Luo, F. Himo, É.A. Enyedy, V.B. Arion, A. Gräslund, J. Inorg. Biochem. 105 (2011) 1422–1431.
[18] C. Stefani, P.J. Jansson, E. Gutierrez, P.V. Bernhardt, D.R. Richardson, D.S. Kalinowski, J. Med. Chem. 56 (2013) 357–370.
[19] D.B. Lovejoy, P.J. Jansson, U.T. Brunk, J. Wong, P. Ponka, D.R. Richardson, Cancer Res. 71 (2011) 5871–5880.
[20] J. Qi, Q. Yao, K. Qian, L. Tian, Z. Cheng, D. Yang, Y. Wang, Eur. J. Med. Chem. 154 (2018) 91–100.
[21] J. Qi, Q. Yao, K. Qian, L. Tian, Z. Cheng, Y. Wang, J. Inorg. Biochem. 186 (2018) 42–50.
[22] P. Chen, T. Hu, Y. Ma, X. Chen, L. Dai, N. Lei, Z. Dong, P. Li, Cancer Res. 7515 (2015).
[23] S. Sakamuru, M.S. Attene-Ramos, M. Xia, Methods Mol. Biol. 1473 (2016) 17–22.
[24] E. Vilventhraraja, T. Klymenko, J. Edelmann, J. Gribben, A. Ivanov, Blood 128 (2016).
[25] G.C. Bullock, C.L. Richardson, V. Schrott, N.D. Gunawardena, T.N. Cole, C.G. Corey, S.S. Shiva, Blood 126 (2015).
[26] A. Sallmyr, Y. Matsumoto, V. Roginskaya, B. Van Houten, A.E. Tomkinson, Cancer Res. 76 (2016) 5431–5441.
[27] A. Di Stefano, S. Frosali, A. Leonini, A. Ettorre, R. Priora, F.C. Di Simplicio, P. Di Simplicio, Biochim. Biophys. Acta 1763 (2006) 214–225.
[28] J. Qi, J. Deng, K. Qian, L. Tian, J. Li, K. He, X. Huang, Z. Cheng, Y. Zheng, Y. Wang, Eur. J. Med. Chem. 134 (2017) 34–42.

[29] J. Qi, Y. Zheng, K. Qian, L. Tian, G. Zhang, Z. Cheng, Y. Wang, J. Inorg. Biochem. 177 (2017) 110–117.
[30] S. Vamadevan, K. Le, C. Bui, R. Mansberg, Clin. Nucl. Med. 42 (2017) 287–288.
[31] B. Dumontel, M. Canta, H. Engelke, A. Chiodoni, L. Racca, A. Ancona, T. Limongi, G. Canavese, V. Cauda, J. Mater. Chem. B 5 (2017) 8799–8813.
[32] P. Wang, M.A. Rahman, Z. Zhao, K. Weiss, C. Zhang, Z. Chen, S.J. Hurwitz, Z.G. Chen, D.M. Shin, Y. Ke, J. Am. Chem. Soc. 140 (2018) 2478–2484.
[33] H. Lu, R.A. Shamanna, J.K. de Freitas, M. Okur, P. Khadka, T. Kulikowicz, P.P. Holland, J. Tian, D.L. Croteau, A.J. Davis, V.A. Bohr, Nat. Commun. 8 (2017) 2039.
[34] A. Hu, J.J. Huang, J.F. Zhang, W.J. Dai, R.L. Li, Z.Y. Lu, J.L. Duan, J.P. Li, X.P. Chen, J.P. Fan, W.H. Xu, H.L. Zheng, Oncotarget 8 (2017) 50747–50760.
[35] W. Xu, B. Wang, M. Yang, Y. Zhang, Z. Xu, Y. Yang, H. Cao, L. Tao, Environ. Toxicol. Pharmacol. 49 (2017) 89–96.
[36] J. Qi, K. Qian, L. Tian, Z. Cheng, Y. Wang, New J. Chem. 42 (2018) 10226–10233.
[37] V. Deswaerte, P. Nguyen, A. West, A.F. Browning, L. Yu, S. Ruwanpura, J. Balic, T. Livis, C. Girard, A. Preaudet, H. Oshima, K.Y. Fung, H. Tye, M. Najdovska, M. Ernst, M. Oshima, C. Gabay, A. Preaudet, Cancer Res. 78 (2017) 1293–1307.
[38] Z. Cao, Q. Yang, H. Yin, Q. Qi, H. Li, G. Sun, H. Wang, W. Liu, J. Li, Apoptosis 22 (2017) 1419–1430.
[39] Z. Feng, W. Zheng, Q. Tang, L. Cheng, H. Li, W. Ni, X. Pan, Apoptosis 22 (2017) 1001–1012.
[40] L.M. Fan, J.M. Li, J. Pharmacol. Toxicol. Methods 70 (2014) 40–47.
[41] R.R. Del, R.J. Barr, B.S. Graham, S. Kaneshiro, Am. J. Dermatopathol. 27 (2005) 259–267.
[42] A. Costa, A. Scholer-Dahirel, F. Mechta-Grigoriou, Semin. Cancer Biol. 25 (2014) 23–32.
[43] H. Huang, C. Liu, X. Fu, S. Zhang, Y. Xin, Y. Li, L. Xue, X. Cheng, H. Zhang, Front. Physiol. 7 (2016) 397.
[44] M.I. Khan, A. Mohammad, G. Patil, S.A. Naqvi, L.K. Chauhan, I. Ahmad, Biomaterials 33 (2012) 1477–1488.
[45] I.S. Woo, H. Jin, E.S. Kang, H.J. Kim, J.H. Lee, K.C. Chang, J.Y. Park, W.S. Choi, H.G. Seo, Cancer Lett. 309 (2011) 190–198.
[46] A.D. Smart, R.A. Pache, N.D. Thomsen, T. Kortemme, G.W. Davis, J.A. Wells, Proc. Natl. Acad. Sci. U. S. A. 114 (2017) E8174–E8183.
[47] S. Kumar, P. Cieplak, Apoptosis 23 (2018) 194–200.